Catalysis Science & Technology

Propane metathesis and hydrogenolysis over titanium hydride catalysts

Journal:	*Catalysis Science & Technology*
Manuscript ID	CY-ART-08-2023-001187
Article Type:	Paper
Date Submitted by the Author:	26-Aug-2023

Complete List of Authors:	Huang, Mengwen; Hokkaido University Tomimuro, Yosuke; Hokkaido University Miyazaki, Shinta; Hokkaido University, Institute for Catalysis Mine, Shinya; National Institute of Advanced Industrial Science and Technology, Research Institute for Chemical Proscess Technology; Hokkaido University, Institute for Catalysis Toyao, Takashi; Hokkaido university, Institute for Catalysis Hinuma, Yoyo; AIST, Kanda, Yasuharu; Muroran Kogyo Daigaku, Kitano, Masaaki; Tokyo Institute of Technology, Materials Research Center for Element Strategy Shimizu, Ken-ichi; Hokkaido University, Catalysis Research Center Maeno, Zen; Kogakuin University, School of Advanced Engineering

ARTICLE

fmonoReceived 00th January 20xx,

Accepted 00th January 20xx

DOI: 10.1039/x0xx00000x

Propane metathesis and hydrogenolysis over titanium hydride catalysts

Mengwen Huang,[a] Yosuke Tomimuro,[a] Shinta Miyazaki,[a] Shinya Mine,[a] Takashi Toyao,[a] Yoyo Hinuma,[b] Yasuharu Kanda,[c] Masaaki Kitano,[d,e] Ken-ichi Shimizu*[a] and Zen Maeno*[f]

Propane metathesis reactions over group 2–5 metal hydrides were investigated. Among the tested metal hydrides, TiH_2 exhibited the highest butane yield as the metathesis reaction product. Fully-hydrogenated TiH_2 are much more active than dehydrogenated TiH and Ti metal. The surface low-valent Ti species over TiH_2 involve propane metathesis reaction. This study is the first example of carbon–carbon bond cleavage and catalytic formation over bulk metal hydrides.

Introduction

Hydrogen-containing compounds such as metal hydrides have been studied in numerous research fields, including energy engineering, electrochemistry, and catalysis owing to their unique chemical and physical properties.[1–6] In the field of catalysis, studies on metal hydride-based catalysts have been much less reported compared to those on metal- and metal oxide-based catalysts, despite the previous reports on the catalysis of metal hydrides for hydrogenation and dehydrogenation of hydrocarbons in the early 1900s.[7–9] Recently, the effectiveness of metal hydrides as catalysts or supports for hydrogenation reactions, including CO_2 to CH_4 and N_2 to NH_3, has been demonstrated by several research groups.[10–15] Both hydride ions and hydrogen vacancies are key in promoting the reactions efficiently or enhancing the catalytic activities of the supported metal species. Although hydrogenation catalysis of metal hydrides has progressed in the studies above, the catalysis for other molecular transformations has rarely been explored.

Alkane metathesis is the catalytic conversion of alkanes into lower and higher ones simultaneously, and is a possible way to upgrade light alkanes. It originated when Burnett and Hughes first discovered the conversion of propane into lower and higher alkanes using a combination of Pt/Al_2O_3 and WO_3/SiO_2.[16] Subsequently, Basset achieved selective conversion of two molecules of propane into ethane and butane, named alkane metathesis, using isolated Ta hydrides on SiO_2 prepared via surface organometallic chemistry (SOMC) techniques.[17] Several monometallic and bimetallic catalyst systems have been developed for alkane metathesis. Monometallic single-site Ta-, Zr-, W-, and Mo-catalyst have been developed by Basset and Copéret via SOMC techniques[18–31]. Bimetallic catalyst systems have been studied using a combination of dehydrogenation/hydrogenation catalysts (supported Pt-based nanoparticles, organometallic Zr and Ti complexes, as well as Pincer-type Ir complexes) and olefin metathesis catalysts (supported WO_3, Re_2O_7, and organometallic W complexes as well as Schrock-type Mo complexes).[32–36] The mechanism of the metathesis reaction over monometallic catalyst systems involves the olefin metathesis reaction on metallocarbene species, formed via H elimination from the corresponding metal-alkyl intermediates.[37] The homologation reaction of alkanes on W films in the copresence of H_2 was also reported where surface methylenes are possible intermediates.[38] Alkane metathesis reactions with bimetallic catalyst systems likely proceed via the following three steps: (i) dehydrogenation of alkanes into the corresponding olefins, (ii) olefin metathesis to generate lower and higher olefins, and (iii) hydrogenation of the generated olefins to form lower and higher alkanes.[33] Regardless of the reaction mechanism and/or pathway, multifunctionality promoting carbon–hydrogen/carbon–carbon bond cleavage and formation is necessary to achieve alkane metathesis reactions, which makes exploring of new catalyst systems challenging.

Herein, we report a propane metathesis reaction over metal hydride catalysts. Among the metal hydrides tested, TiH_2 afforded the highest yield of butane as a metathesis product, although lower alkanes, such as ethane and methane, were formed through hydrogenolysis. This study demonstrates the catalytic potential of metal hydrides for carbon–carbon bond cleavage and formation.

[a] Institute for Catalysis, Hokkaido University, N-21, W-10, Sapporo 001-0021, Japan.
[b] Department of Energy and Environment, National Institute of Advanced Industrial Science and Technology, 1-8-31, Midorigaoka, Ikeda 563-8577, Japan.
[c] Applied Chemistry Research Unit, College of Information and Systems, Graduate School of Engineering, Muroran Institute of Technology, 27-1 Mizumoto, Muroran 050-8585, Japan.
[d] Laboratory for Materials and Structures, Institute of Innovative Research, Tokyo Institute of Technology, Midori, Yokohama 226-8503, Japan
[e] Advanced Institute for Materials Research (WPI-AIMR), Tohoku University, Sendai 980-8577, Japan
[f] School of Advanced Engineering, Kogakuin University, 2665-1, Nakano-cho, Hachioji, 192-0015, Japan

† Electronic Supplementary Information (ESI) available: Details of gas composition and analysis of catalytic reaction, TEM images, Results of control experiments. See DOI: 10.1039/x0xx00000x

Experimental

General

TiH_2 (powder, < 45 μm, purity: >99%) was purchased from Kojundo Chemical Laboratory Co.,ltd. TiO_2 (anatase, ST-01) and $BaTiO_3$ (particle size ~100 nm) were kindly supplied from ISHIHARA SANGYO KAISHA, LTD. and Sakai Chemical Industry Co., Ltd., respectively. TiN (powder, < 3 μm) was obtained from Sigma-Aldrich Co., LLC. Ti metal was prepared by dehydrogenation of TiH_2 under H_2 flow at 500 ˚C, and then used for the reaction. Other group 4 and 5 metal hydrides, ZrH_2 (powder, Mitsuwa Chemical Co.,Ltd.), HfH_2 (powder, < 75 μm, purity: >99.5%, Goodfellow), and V_2H (powder, < 75 μm, Kojundo Chemical Laboratory Co., ltd. were commercially obtained. The group 3 metal hydrides (ScH_2, YH_3, and LaH_3) were prepared by reacting metal chips (purity: >99.9%, RARE METALLIC Co.,LTD.) in an H_2 atmosphere (1.5 MPa) at various temperatures (400 ˚C for ScH_2 and YH_3, room temperature for LaH_3) for 4 h. The ball-milled metal hydrides were prepared using a Fritsch P-6 planetary ball mill. For example, TiH_2 (1 g) was milled together in an ZrO_2 pot (80 mL) with zirconia balls (ø5 mm, 100 g). The milling conditions were 200 rpm with a 1-min interval after every 9 min of milling for 1, 12, and 24 h. All the ball milling was performed without exposure to air and the obtained samples were stored in a glove box filled with Ar.

Propane metathesis and hydrogenolysis reactions

Propane metathesis and hydrogenolysis reactions over metal hydrides were carried out using an autoclave (10 cm^3). A powder of metal hydride (50 mg) was added to the autoclave in a glove box filled with Ar, and then the inner gas was replaced with propane (C_3H_8) at room temperature. The mixture was stirred magnetically at elevated temperatures. After the reaction, the reactor was cooled to room temperature, and the gas phase products were analyzed using a gas chromatography (GC, Shimadzu GC-14B) with a flame ionization detector (FID) and a Unipack S column. The compositions of a series of gas products were determined on the basis of effective carbon numbers and GC areas. Note that the detailed structures of pentanes and hexanes were not analyzed. The propane conversion, product selectivity, yields of butane (Y_{C4H10}) and methane (Y_{CH4}), were calculated from the gas compositions. Coke formation was negligible as indicated by temperature programmed oxidation (TPO) of the used TiH_2 catalyst. The total formation amount of butane was determined by the volume of autoclave, the compositions of *iso*-/*n*-butane, and the amount of catalyst. The equations for calculation of conversion, yields, selectivity, and formation amounts are described in ESI.

Characterizations

X-ray photoelectron spectroscopy (XPS) spectra were measured on a JEOL JPC-9010MC spectrometer having a modified UHV chamber employing Mg Kα radiation. Charge correction was referenced using the O 1s peak at 532.0 eV. Scanning electron microscopy (SEM) measurement were conducted using JEOL JSM-7400F while transmission electron microscopy (TEM) measurement was performed using JEOL JEM-2100F. *In situ* X-ray diffraction (XRD) measurement was conducted using a Cu Kα radiation source (Rigaku Ultima IV, Rigaku Corporation, Japan). XRD patterns were obtained while heating ball-milled TiH_2 from room temperature to 400 °C under He flow (100 mL/min). Note that the ball-milled TiH_2 was transferred to the chamber without exposure to air for XPS measurement whereas TiH_2 samples after exposure to air were used for SEM, TEM, and XRD measurements. For H_2 temperature programmed desorption (TPD) measurement, ball-milled TiH_2 was loaded into U-tube quartz reactor (attached with 4-way valve) without exposure to air and set in the electronic heating furnace. The temperature was increased with a ramping rate of 10 °C/min. The generated H_2 was analyzed by an online mass spectrometry using BELLMASS II (MicrotracBEL).

Results and Discussion

Propane metathesis and hydrogenolysis over metal hydrides

First, we studied propane metathesis reactions using 1 h ball-milled metal hydrides (MH_x_BM1h) at 300 °C under 1 atm of C_3H_8 using a batch reactor without exposure to the air. The butane (C_4H_{10}) yield, Y_{C4H10}, was calculated based on the gas composition of *n*-/*iso*-C_4H_{10} and other alkanes to evaluate propane metathesis catalysis because propane hydrogenolysis reaction also occurred as a side reaction. The metathesis selectivity was estimated from Y_{C4H10} and Y_{CH4} as indicators of the metathesis and hydrogenolysis reactions, respectively, because ethane (C_2H_6) is likely formed in both reactions. In this system, coke formation almost did not occur, as indicated by TPO measurements, where CO_2 was scarcely detected, verifying the above calculation based on the gas composition. The results are summarized in Table 1. A comparison of the total amount of C_4H_{10} formed, the product selectivity, and the metathesis selectivity is shown in Fig. 1.

Among the tested metal hydrides, group 4 metal hydrides, such as TiH_2, ZrH_2, and HfH_2, exhibited higher Y_{C4H10} values (entries 1–3) than group 2 (MgH_2 and CaH_2), 3 (ScH_2, YH_3, and LaH_3), and 5 (V_2H) metal hydrides (entries 4–9). In particular, TiH_2 exhibited the highest Y_{C4H10} (3.0%) at 28.8% of C_3H_8 conversion (entry 1). Note that trace amounts of pentane (C_5H_{12}) and hexane (C_6H_{14}) were also formed as metathesis reaction products, and possible olefins such as ethylene (C_2H_4) and butene (C_4H_8) were not detected (for detailed results, see Table S1 in ESI). The metathesis selectivity for TiH_2 was determined to be 10.4%, which is the highest among the tested metal hydrides. When Ti metal, TiN, TiO_2, and $BaTiO_3$ were used instead of TiH_2 (entries 11–14 vs. entry 10), the C_3H_8 conversion and Y_{C4H10} were much lower, confirming that propane metathesis reactions occur uniquely over TiH_2. In the literature, the formation of metal-alkyl intermediates is one of the important elementary steps to promote alkane metathesis reactions.[37] The smaller difference in electronegativity between metal and carbon elements is generally more favourable for the formation of corresponding covalent metal-carbon bonds. One of the possible reasons for higher butane yield for TiH_2 might be the higher electronegativity of Ti than other metal elements except for V although it is still difficult to conclude the origin of higher performance of TiH_2 owing to the complexity of reaction mechanism and/or pathway of propane metathesis over metal hydrides (see below).

The effects of reaction conditions on the amount of C_4H_{10} formed and metathesis selectivity in the propane metathesis reaction over TiH_2 were also studied. TiH_2_BM12h was used in these experiments. The reaction of C_3H_8 hardly occurred at T =

Table 1 Propane metathesis reaction over metal hydrides and other materials.[a] Detailed results including compositions of other gas products are summarized in Table S1 (See ESI).

Entry	Catalyst[b]	C_3H_8 conversion[c] / %	Metathesis selectivity[d] / %	Y_{C4H10}[c] / %
1	TiH_2	28.8	10.4	3.0
2	ZrH_2	37.8	3.4	1.3
3	HfH_2	34.4	2.0	0.7
4	MgH_2	2.3	5.0	0.1
5	CaH_2	3.2	6.0	0.2
6	ScH_2	55.2	0.6	0.3
7	YH_3	18.3	2.7	0.5
8	LaH_3	6.9	1.0	<0.1
9	V_2H	47.4	1.2	0.6
10	Ti metal	<0.1	n.a.[e]	n.a.[e]
11	TiN	8.8	n.a.[e]	n.a.[e]
12	TiO_2	0.5	19.5	0.1
13	$BaTiO_3$	2.6	9.8	0.3

[a]Reaction conditions: 50 mg of catalyst, 1 atm of C_3H_8, 300 °C, 24 h. [b]The ball-milled metal hydride was prepared using a Fritsch P-6 planetary ball mill, and subsequently used for the reactions without exposure to air. [c]The conversion and yield were calculated based on the gas composition after the reaction using gas chromatography with FID (FID-GC). For the details, see ESI. [d]Estimated based on the following equation: $Y_{C4H10}/(Y_{C4H10} + Y_{CH4})$. For the details, see ESI. [e]Not available.

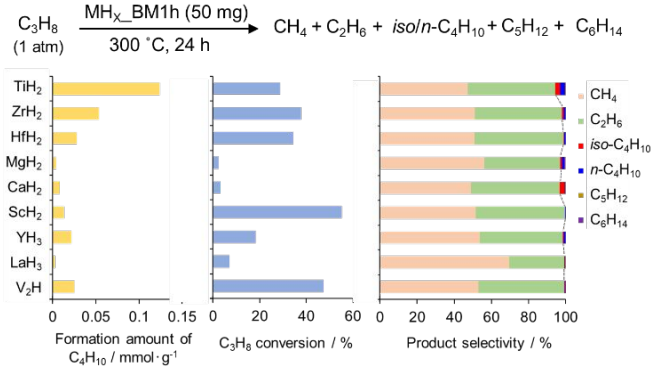

Fig. 1 Formation amount of C_4H_{10} (*iso*/*n*-C_4H_{10}), C_3H_8 conversion, and product selectivity in the propane metathesis and hydrogenolysis over metal hydrides.

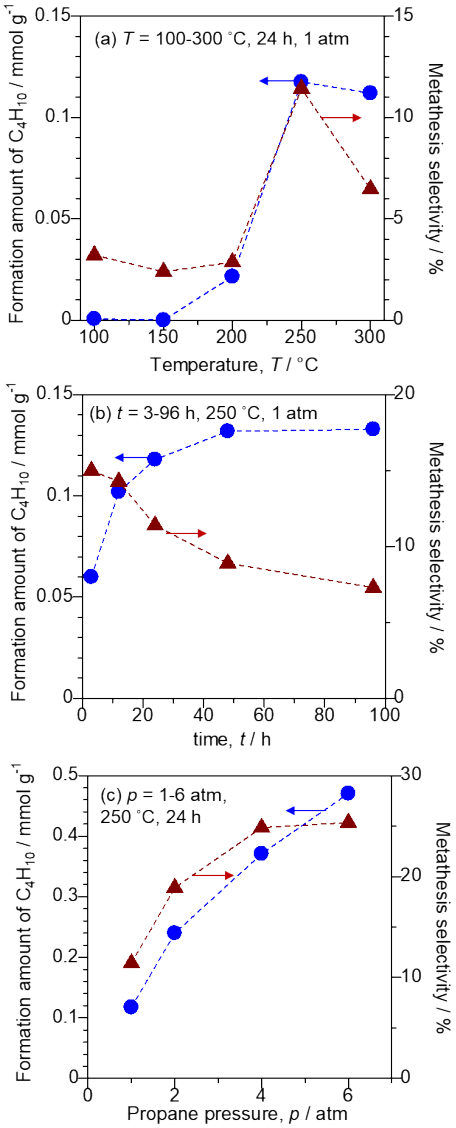

Fig. 2 Effect of (a) temperature (*T*), (b) time (*t*), and (c) pressure (*p*) on the total formation amount of C_4H_{10} and in propane metathesis over TiH_2_BM12h. Blue circles and brown triangles indicate formation amount of C_4H_{10} (left axis) and metathesis selectivity (right axis).

100 °C (*T* denotes the reaction temperature), whereas C_4H_{10} was not detected. The metathesis reaction occurred when *T* was increased to 150 °C (Fig. 2a). The amount of C_4H_{10} formed increased from 0.022 to 0.118 mmol · g^{-1} as *T* increased from 150 to 250 °C. A further increase in *T* to 300 °C did not improve the amount of C_4H_{10} formed (0.112 mmol · g^{-1}). The highest selectivity was observed at 250 °C. Regarding the reaction time dependency, the formation amount increased with increasing reaction time (*t*) to 48 h and then leveled off after 96 h (Fig. 2b). The metathesis selectivity decreased monotonically from 15.0% to 7.3%. The increase in C_3H_8 pressure (*p*) not only enhanced the amount of C_4H_{10} formed from 0.117 to 0.471 mmol · g^{-1} but also improved the metathesis selectivity from 11.4% to 25.3% (Fig. 2c). Under the optimized reaction conditions (*T* = 250 °C, *p* = 6 atm, *t* = 96 h), the formation amount was 0.47 mmol · g^{-1}. The turnover number, based on the number of surface Ti–H units estimated from the specific surface area[39] (see below) and the model structure of the most-stable TiH_2 (101) surface,[40] was determined to be 4.0, indicating that the propane metathesis reaction over TiH_2 occurs catalytically.

Possible active Ti species on titanium hydrides

The effect of pretreatment on propane metathesis catalysis was investigated (Table 2). TiH_2 without ball milling (TiH_2_as received) exhibited lower C_3H_8 conversion (20.6% vs. 28.8%) and worse Y_{C4H10} (1.3% vs. 3.0%) than TiH_2_BM1h (entry 1 vs. Entry 2). When TiH_2_BM1h was exposed to air and used for the reaction (TiH_2_BM1h-Air), both the C_3H_8 conversion and Y_{C4H10} significantly decreased from 28.8% to 4.4% and from 3.0% to 0.1%, respectively (entry 2 vs. entry 5). The XPS measurements of TiH_2_BM1h and BM1h-Air (Fig. 3) revealed that exposure to air induced surface oxidation of TiH_2_BM1h to afford mainly oxidized Ti(IV) species, indicating that the surface low-valent Ti species involves propane metathesis reaction. We attempted to

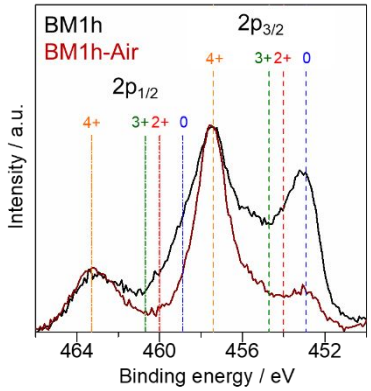

Fig. 3 XPS spectrum for Ti 2p region of TiH_2_BM1h before (black) and after (BM1h-Air, brown) exposure to air.

enhance Y_{C4H10} by extending the ball-milling time from 1 to 12 h and 24 h (entries 3 and 4, respectively). Although the surface area value increased monotonically from 5.2 to 6.7, 7.2 $m^2 \cdot g^{-1}$,[39] the extension of ball-milling time decreased the metathesis selectivity (7.7% and 3.2% for TiH_2_BM12h and BM24h, respectively), resulting in worse Y_{C4H10} (2.6% and 1.7%). These results differ from propane dehydrogenation into propylene using TiH_2, where the reaction rate increased monotonically with increasing ball-milling time.[39] The SEM images of a series of TiH_2 (as received, BM1h, and BM24h) showed that the ball-milling treatment changed their surface texture from flat to bumpy (Fig. S1 in ESI), which might negatively affect the active surface of TiH_2.

TiH_2_BM1h before and after the reaction (at 300 °C for 24 h) were also characterized by XRD and XPS measurements. Note that the samples were used for the measurement without exposure to air. In the XRD measurement, the diffraction pattern of TiH_2 was largely maintained while a few diffraction peaks ascribed to Ti and TiH appeared (Fig. S2), indicating that the part of TiH_2 was dehydrogenated. The XPS spectrum showed that the low-valent Ti species increased after the reaction (Fig. S3), which is not inconsistent with the formation of Ti and TiH.

Table 2 Effect of pretreatment on propane metathesis reaction over TiH_2.[a]

Entry	Pretreatment	Surface area[d] / $m^2 \cdot g^{-1}$	C_3H_8 conversion[f] / %	Metathesis selectivity[f] / %	Y_{C4H10}[f] / %
1	None (as received)	1.2	20.6	6.1	1.3
2	BM1h[b]	5.2	28.8	10.4	3.0
3	BM12h[b]	6.7	34.1	7.7	2.6
4	BM24h[b]	7.2	53.8	3.4	1.7
5	BM1h-Air[c]	n.a.[e]	4.4	2.2	0.1

[a]Reaction conditions: 50 mg of catalyst, 1 atm of C_3H_8, 300 °C, 24 h. [b]The ball-milled TiH_2 was prepared using a Fritsch P-6 planetary ball mill, and subsequently used for the reactions without exposure to air. [c]The ball-milled sample was exposed to air at room temperature (25 °C) overnight, and thereafter used for the reaction experiment. [d]The data were reported in our previous study.[39] [e]Not available. [f]The details for calculation are described in ESI.

Our recent study on propane dehydrogenation over titanium hydrides revealed that TiH_2 was converted into partially dehydrated TiH_X (X = 1 or 0.85) or Ti metal in the presence or absence of H_2 cofeeding at 450 °C, respectively, where TiH_X is more active than Ti metal for dehydrogenation.[39] To gain insight into the structure of active titanium hydrides, TiH_2_BM1h was treated under He flow at different temperatures (100–400 °C) to prepare partially dehydrogenated titanium hydrides and thereafter used for the propane metathesis reaction. The *in situ* XRD measurements of TiH_2 under He flow revealed that the diffraction pattern of TiH_2 disappeared, and diffraction peaks assignable to TiH appeared at 300 °C. At 400 °C, the diffraction patterns of TiH_2 and TiH were hardly observed, and broad peaks derived from Ti metal appeared (Fig. 4a).

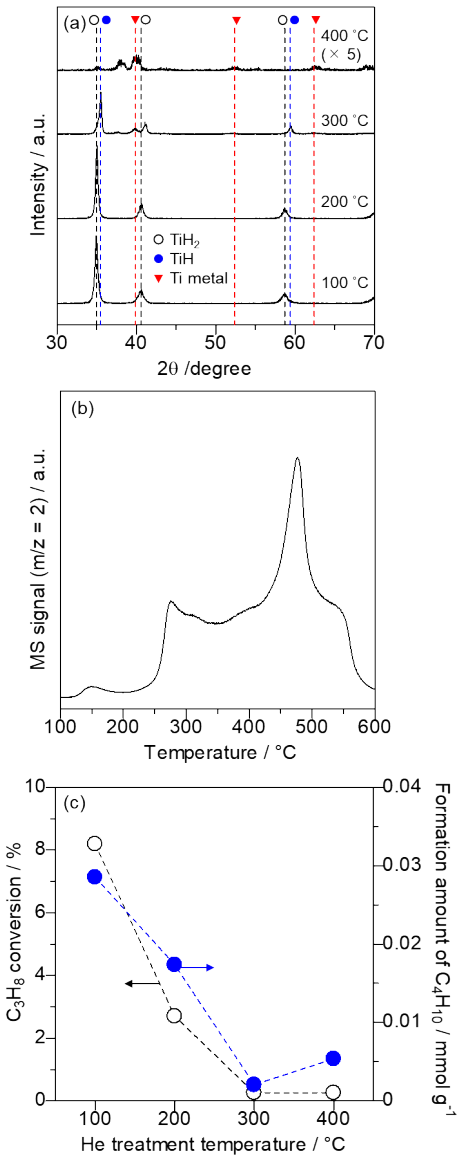

Fig. 4 (a) *In situ* XRD patterns of the TiH_2_BM1h treated with He at different temperature. TiH_2_BM1h after exposure to air was used for *in situ* XRD measurement. (b) H_2 TPD profile of TiH_2_BM1h for m/z = 2. The sample was trasferred to the reactor without exposure to air and then the TPD experiment was conducted. (c) The effect of He treatment temeprature on C_3H_8 conversion and formation amount of C_4H_{10} in propane metathesis over He-treated TiH_2_BM1h. The He treated sample was used for the reaction without exposure to air.

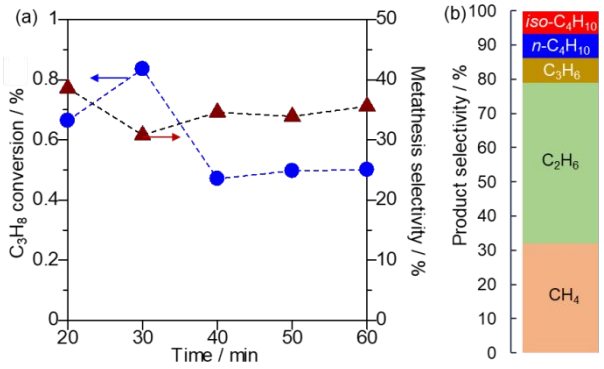

Fig. 5 (a) C_3H_8 conversion and metathesis selectiity in propane metathesis over TiH_2_BM1h using flow-type reactor (Reaction conditions: 0.2 g of TiH_2_BM1h, 10 mL/min of 10% C_3H_8, 250 °C). (b) Product selectivity in the reaction at 30 min.

The H_2 TPD measurement showed that the dehydrogenation of TiH_2 started at 100 °C, and the main desorption peak was observed in the range of 300–400 °C (Fig. 4b), which is consistent with the results of *in situ* XRD measurements. In propane metathesis reactions, TiH_2_BM1h treated at 100 and 200 °C exhibited activity, whereas both the C_3H_8 conversion and formation amount of C_4H_{10} significantly decreased with increasing He pretreatment temperature to 300 and 400 °C (Fig. 4c). These results demonstrate that fully hydrogenated titanium hydrides are more active than partially dehydrogenated ones for propane metathesis. The most suitable temperature for achieving high performance (250 °C, Fig. 2a) was lower than the temperature range (300-400 °C, Fig. 4b) for the first main H_2 desorption peak in the TPD, which is consistent with this consideration. Combined with the XPS results (Fig. 3, see above), the low-valent Ti species generated by desorption of adjacent lattice hydrogen anions on crystalline TiH_2 surface are plausible active sites.

To gain further insight into the reaction mechanism and/or pathway, we also investigated the propane metathesis reaction over the ball-milled TiH_2 (TiH_2_BM1h) using a flow-type reactor at 250 °C. Under an Ar atmosphere in a glove box, 200 mg of TiH_2_BM1h was loaded into a U-shaped quartz reactor equipped with a 4-way valve. The reactor was removed, taking care to ensure no exposure to air, and placed in an electric furnace to conduct the reaction (Fig. S4). *n*-/*iso*-C_4H_{10} were formed in considerable selectivity (13.8%, Fig. 5b) at 250 °C although the conversion value (0.83%, Fig. 5a) was much lower than those in the experiments using batch-type reactor owing to much shorter contact time and the hydrogenolysis products (C_2H_6 and CH_4) were formed as main products. The C_3H_8 conversion and metathesis selectivity values were maintained for 60 min. Notably, C_3H_6 was also formed as a C_3H_8 dehydrogenation product. However, higher and lower olefins were hardly detected. This is in sharp contrast to the results in propane metathesis using reported catalyst systems where C_4H_8 and C_2H_4 were formed with C_3H_6,[37] which indicates that further investigations, including spectroscopic and theoretical studies, are still required to elucidate the reaction mechanisms and/or pathways in our catalyst systems.

Conclusions

In conclusion, we developed a propane metathesis catalysis of metal hydrides. Group 3 metal hydrides afforded higher yields of C_4H_{10} than groups 2, 4, and 5 metal hydrides. The highest C_4H_{10} yield was obtained using ball-milled TiH_2, although considerable amounts of C_2H_6 and CH_4 were formed through direct hydrogenolysis in the absence of a gaseous H_2 source. TiH_2 is much more active than partially dehydrogenated titanium hydrides such as TiH for propane metathesis. To the best of our knowledge, this is the first example of bulk metal hydride system that promotes alkane metathesis reactions.

Acknowledgements

This study was financially supported by KAKENHI (Grant No. JP20H02518, JP20KK0111, JP21H04626, and JP23H01765) from the Japan Society for the Promotion of Science (JSPS) and KAKENHI on Innovative Areas “Hydrogenomics” (No. JP21H00019 and JP21H00012). This study was also supported by the JST-CREST project JPMJCR17J3, the JST-SPRING project JPMJSP2119, and the Joint Usage/Research Center for Catalysis. The authors thank Shuhei Shimoda (Institute for Catalysis, Hokkaido University) for his technical support in TEM and SEM measurement.

Author Contributions

Z.M. conceived the idea of study and supervised the conduct of this study. M.H., Y.T., and S.Mine performed the experiments for catalyst preparation and catalytic reactions. S.Miyazaki and Y.K. conducted the XPS and *in situ* XRD measurements, respectively. Y.H. analyzed the experimental data based on computational study. M.K. synthesized a part of metal hydrides. M.H. also wrote the draft, and T.T., K.S., and Z.M. critically reviewed it. All authors approved the final version of the manuscript to be published.

Conflicts of interest

There are no conflicts to declare.

Notes and references

1 K. Fukutani, J. Yoshinobu, M. Yamauchi, T. Shima and S. Orimo, *Catal. Lett.*, 2022, **152**, 1583-1597.
2 H. Hosono and M. Kitano, *Chem. Rev.*, 2021, **121**, 3121–3185.
3 H. Kageyama, K. Hayashi, K. Maeda, J. P. Attfield, Z. Hiroi, J. M. Rondinelli and K. R. Poeppelmeier, *Nat. Commun.*, 2018, **9**, 772.
4 C. Copéret, D. P. Estes, K. Larmier and K. Searles, *Chem. Rev.*, 2016, **116**, 8463–8505.
5 A. Schneemann, J. L. White, S. Kang, S. Jeong, L. F. Wan, E. S. Cho, T. W. Heo, D. Prendergast, J. J. Urban, B. C. Wood, M. D. Allendorf and V. Stavila, *Chem. Rev.*, 2018, **118**, 10775–10839.
6 J. Guo and P. Chen, *Acc. Chem. Res.*, 2021, **54**, 2434–2444.
7 S. Weller and L. Wright, *J. Am. Chem. Soc.*, 1954, **76**, 5302–5305.
8 L. Wright and S. Weller, *J. Am. Chem. Soc.*, 1954, **76**, 5305–5308.
9 R. N. Pease and L. Stewart, *J. Am. Chem. Soc.*, 1925, **47**, 2763–2766.

10 M. Kitano, J. Kujirai, K. Ogasawara, S. Matsuishi, T. Tada, H. Abe, Y. Niwa and H. Hosono, *J. Am. Chem. Soc.*, 2019, **141**, 20344–20353.
11 M. Hattori, S. Iijima, T. Nakao, H. Hosono and M. Hara, *Nat. Commun.*, 2001, **11**, 2020.
12 Y. Kobayashi, Y. Tang, T. Kageyama, H. Yamashita, N. Masuda, S. Hosokawa and H. Kageyama, *J. Am. Chem. Soc.*, 2017, **139**, 18240–18246.
13 Y. Cao, A. Saito, Y. Kobayashi, H. Ubukata, Y. Tang and H. Kageyama, *ChemCatChem*, 2021, **13**, 191–195.
14 S. Kato, S. K. Matam, P. Kerger, L. Bernard, C. Battaglia, D. Vogel, M. Rohwerder and A. Züttel, *Angew. Chem. In. Ed.*, 2016, **55**, 6028–6032.
15 P. Wang, F. Chang, W. Gao, J. Guo, G. Wu, T. He and P. Chen, *Nat. Chem.*, 2017, **9**, 64–70.
16 R. L. Burnett and T. R. Hughes, *J. Catal.*, 1973, **31**, 55–64.
17 V. Vidal, A. Theolier, J. Thivolle-Cazat and J.-M. Basset, *Science*, 1997, **276**, 99–102.
18 E. le Roux, M. Taoufik, C. Copéret, A. de Mallmann, J. Thivolle-Cazat, J.-M. Basset, B. M. Maunders and G. J. Sunley, *Angew. Chem. Int. Ed.*, 2005, **44**, 6755–6758.
19 O. Maury, L. Lefort, V. Vidal, J. Thivolle-Cazat and J.-M. Basset, *Angew. Chem. Int. Ed.*, 1999, **38**, 1952–1955.
20 C. Thieuleux, A. Maraval, L. Veyre, C. Copéret, D. Soulivong, J.-M. Basset and G. J. Sunley, *Angew. Chem. Int. Ed.*, 2007, **46**, 2288–2290.
21 K. C. Szeto, L. Hardou, N. Merle, J.-M. Basset, J. Thivolle-Cazat, C. Papaioannou and M. Taoufik, *Catal. Sci. Technol.*, 2012, **2**, 1336–1339.
22 F. Blanc, J. Thivolle-Cazat, J.-M. Basset and C. Copéret, *Chem. Eur. J.*, 2008, **14**, 9030–9037.
23 D. Soulivong, C. Copéret, J. Thivolle-Cazat, J.-M. Basset, B. M. Maunders, R. B. A. Pardy and G. J. Sunley, *Angew. Chem. Int. Ed.*, 2004, **43**, 5366–5369.
24 Y. Chen, E. Abou-Hamad, A. Hamieh, B. Hamzaoui, L. Emsley and J.-M. Basset, *J. Am. Chem. Soc.*, 2015, **137**, 588–591.
25 F. Rataboul, M. Chabanas, A. de Mallmann, C. Copéret, J. Thivolle-Cazat and J.-M. Basset, *Chem. Eur. J.*, 2003, **9**, 1426–1434.
26 W. Wackerow, Z. Thiam, E. Abou-Hamad, W. al Maksoud, M. N. Hedhili and J.-M. Basset, *J. Phys. Chem. C*, 2021, **125**, 12819–12826.
27 W. Wackerow, M. K. Samantaray and J.-M. Basset, *ChemCatChem*, 2020, **12**, 5627–5631.
28 J.-M. Basset, C. Copéret, L. Lefort, B. M. Maunders, O. Maury, E. le Roux, G. Saggio, S. Soignier, D. Soulivong, G. J. Sunley, M. Taoufik and J. Thivolle-Cazat, *J. Am. Chem. Soc.*, 2005, **127**, 8604–8605.
29 E. le Roux, M. Chabanas, A. Baudouin, A. de Mallmann, C. Copéret, E. A. Quadrelli, J. Thivolle-Cazat, J.-M. Basset, W. Lukens, A. Lesage, L. Emsley and G. J. Sunley, *J. Am. Chem. Soc.*, 2004, **126**, 13391–13399.
30 G. Saggio, M. Taoufik, J.-M. Basset and J. Thivolle-Cazat, *ChemCatChem*, 2010, **2**, 1594–1598.
31 N. Maity, S. Barman, E. Callens, M. K. Samantaray, E. Abou-Hamad, Y. Minenkov, V. D'Elia, A. S. Hoffman, C. M. Widdifield, L. Cavallo, B. C. Gates and J.-M. Basset, *Chem. Sci.*, 2016, **7**, 1558–1568.
32 Z. Huang, E. Rolfe, E. C. Carson, M. Brookhart, A. S. Goldman, S. H. El-Khalafy and A. H. R. MacArthur, *Adv. Synth. Catal.*, 2010, **353**, 125–135.
33 A. S. Goldman, A. H. Roy, Z. Huang, R. Ahuja, W. Schinski and M. Brookhart, *Science*, 2006, **312**, 257–261.
34 X. Jia, C. Qin, T. Friedberger, Z. Guan and Z. Huang, *Sci. Adv.*, 2016, **2**, e1501591.
35 M. K. Samantaray, S. Kavitake, N. Morlanés, E. Abou-Hamad, A. Hamieh, R. Dey and J.-M. Basset, *J. Am. Chem. Soc.*, 2017, **139**, 3522–3527.
36 M. K. Samantaray, R. Dey, S. Kavitake, E. Abou-Hamad, A. Bendjeriou-Sedjerari, A. Hamieh and J.-M. Basset, *J. Am. Chem. Soc.*, 2016, **138**, 8595–8602.
37 J.-M. Basset, C. Copéret, D. Soulivong, M. Taoufik and J. Thivolle-Cazat, *Acc. Chem. Res.*, 2010, **43**, 323–334.
38 C. O'Donohoe, J. K. A. Clarke, and J. J. Rooney. *J. Chem. Soc., Chem. Commun.*, 1979, **15**, 648-649.
39 S. Yasumura, Y. Wen, T. Toyao, Y. Kanda, K. Shimizu and Z. Maeno, *Chem. Lett.*, 2022, **51**, 88–90.
40 Y. Hinuma, S. Mine, T. Toyao, Z. Maeno and K. Shimizu, *Phys. Chem. Chem. Phys.*, 2021, **23**, 16577–16593.